



# Characterizing spatially variable water table depths in a disturbed Zoige peatland watershed

Zhiwei Li<sup>a,b</sup>, Peng Gao<sup>c,\*</sup>

<sup>a</sup> State Key Laboratory of Water Resources and Hydropower Engineering Science, Wuhan University, Wuhan 430072, China

<sup>b</sup> School of Hydraulic Engineering, Changsha University of Science & Technology, Changsha 410114, China

<sup>c</sup> Department of Geography, Syracuse University, Syracuse, NY 13244, USA

## ARTICLE INFO

### Keywords:

Water table depth  
Zoige peatland watershed  
Peat depth  
Spatiotemporal variation

## ABSTRACT

Understanding spatial variability of water table depth (WTD) in larger peatland area is crucial for peat conservation. This study investigated spatial patterns of WTDs in a peatland watershed of about 0.151 km<sup>2</sup>, located in the Zoige basin of the Qinghai-Tibet Plateau, China. Using conventional dipwells, we measured WTDs on 5/17/2017, 5/20/2017, 5/23/2017, 7/17/2017, and 9/18/2017 at 114, 103, 105, 77, and 81 locations, as well as peat depths (*H*) and elevations at 119 and 831 locations over the watershed, respectively. Then, we performed hotspot analysis and Geographically Weighted Regression (GWR) modeling, showing (1) highly localized spatial patterns of WTDs, *H*, and *S* (slope gradient, calculated from elevations), and (2) the area that had statistically significant local coefficients for *H* ranged between 51 and 57% of the total watershed area, while that for *S* was only < 11%. These complex spatial patterns of WTDs were further illustrated by our results of examining WTD changes in the lateral and longitudinal directions for two types of channels, deep gullies whose beds are deep and cut through the peat layer and shallow artificial ditches. The findings suggested that spatial and temporal changes of WTDs at the watershed scale may only be examined by collecting *in situ* samples, which may be achieved using an efficient sampling method provided in this study.

## 1. Introduction

As an essential component of the peatland hydrologic functioning, water table depth (WTD) directly affects runoff generation, plant production, and carbon dynamics in peatland (Carlson et al., 2015; Holden et al., 2011; Labadz et al., 2010; Lou et al., 2014; Smiljanic et al., 2014). However, WTD in peatlands varies both in space and time. Temporal changes in WTD are mainly caused by different hydrological processes between rainfall and inter-rain periods. During rainfall, water table rises fast and often reaches the ground surface (Daniels et al., 2008; Evans et al., 1999). As such, much of the precipitation turns into surface runoff quickly, generating flashy hydrographs (Holden and Burt, 2003a; Holden et al., 2006). In inter-rain periods, the water table is relatively low and varies spatially, depending on the paths of macropore and/or pipe flow (Allott et al., 2009; Daniels et al., 2008; Holden and Burt, 2002; Prat-Guitart et al., 2017; Wallage and Holden, 2011). Spatially, WTD can be affected by local topography (Allott et al., 2009; Holden et al., 2006; Luscombe et al., 2016) and artificial drains and natural gullies (Holden et al., 2004; Holden et al., 2011; Ramchunder et al., 2009; Sikstrom and Hokka, 2016). In many studies on feedback

mechanisms between water table and physical properties of peats such as hydraulic conductivity and peat volume (Clymo, 2004; Glaser et al., 1981; Holden et al., 2006; Whittington and Price, 2006), WTD variability was indirectly reflected in their results, though spatial and temporal variations of WTDs were not their main focuses.

While WTD values are commonly obtained by *in situ* sampling in peatlands, their variability has primarily been investigated from two different, but interrelated perspectives. First is spatial and/or temporal variations of WTDs over a small area or at individual locations of peatlands. Spatially variable WTDs were examined by taking regularly spaced samples from peat plots of no > 2500 m<sup>2</sup> (Holden and Burt, 2003b; Holden et al., 2006). Allott et al. (2009) took samples from > 15 sites, each of which contained around 21 samples within a 30 × 30 m area. By collecting WTDs from individual locations along transects representing intact, drained, and blocked peatlands respectively, Holden et al. (2011) illustrated differences of mean WTDs and their temporal trends among these sites.

Second is variable impacts of artificial ditches and natural gullies on WTD variations (Allott et al., 2009; Holden et al., 2011; Luscombe et al., 2016). Allott et al. (2009) showed that (i) WTDs decreased away

\* Corresponding author.

E-mail address: [pegao@maxwell.syr.edu](mailto:pegao@maxwell.syr.edu) (P. Gao).

<https://doi.org/10.1016/j.jher.2020.01.004>

Received 2 May 2019; Received in revised form 14 January 2020; Accepted 17 January 2020

Available online 21 January 2020

1570-6443/ © 2020 International Association for Hydro-environment Engineering and Research, Asia Pacific Division. Published by Elsevier B.V. All rights reserved.

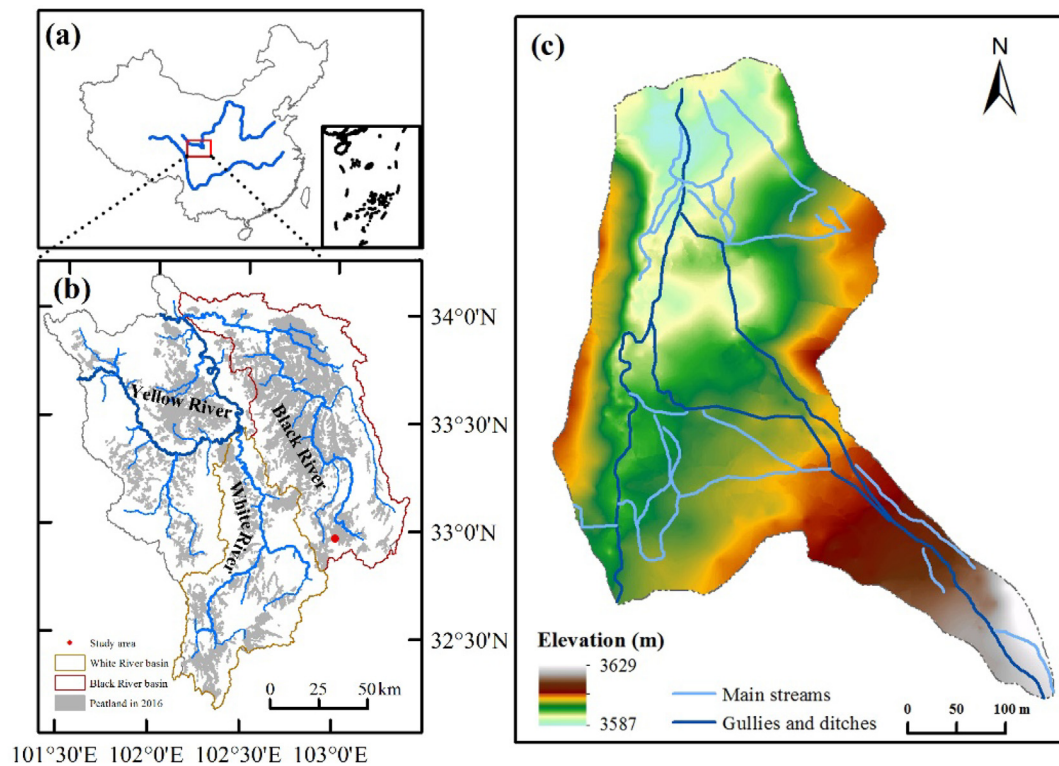


**Fig. 1.** Geographic location and geomorphological structure of the study watershed. (a) Geographic location of the Zoige basin; (b) Distribution of peatland in the Zoige basin and the position of the study watershed, which is represented by the red dot, because its area is < 0.0008% of the area of the entire Zoige basin; (c) The detailed study watershed. (For interpretation of the references to colour in this figure legend, the reader is referred to the web version of this article.)

from a gully or ditch (i.e. distance decay effect); and (ii) increased downslope of a gully or ditch, though the trend was weak. This and other studies revealed that the impact of ditches and gullies on WTDs is generally limited to the peat about 5 to 8 m away from them (Allott et al., 2009; Boelter, 1972; Price et al., 2003). Based on temporally averaged WTDs, Holden et al. (2011) and Luscombe et al. (2016) showed that the distance decay effect existed on the downslope sides of ditches running across slopes, but did not emerge on the upslope sides. Other studies indicated that water table fluctuated greater in the disturbed peatlands than in the intact ones (Daniels et al., 2008; Holden et al., 2006; Wilson et al., 2010).

Clearly, as the spatial scale increases, variability of WTDs becomes more complex and harder to quantify, challenging the need of determining water storage capacity when constructing water budget for peatlands and modeling runoff production at the watershed scale (Luscombe et al., 2016; McCarter and Price, 2013; Shi et al., 2015; Van Seters and Price, 2001). Therefore, understanding spatial and temporal changes of WTDs at the watershed scale in peatlands is critical for unveiling hydrological processes in peatland watersheds and hence for peatland restoration and management. However, achieving this requires answering three questions

Can spatial and temporal variability of WTDs at the watershed scale be characterized by two environmental metrics, slope gradients ( $S$ ) and peat depths ( $H$ )? Although the spatial variation of WTDs are affected by local topography even in small areas (Holden et al., 2006; Luscombe et al., 2016), it is not clear whether it still holds at larger scales because the micro-scale morphologic units, such as pools, peat lawns, and ridges (Whittington and Price, 2006), may give way to regional slope gradients in controlling surface runoff and subsurface flow.

What is the appropriate sampling strategy for obtaining limited data that can sufficiently represent spatial variations of WTDs within a peatland watershed? Perhaps because the sampling plots in previous studies were generally small, which were 900 m<sup>2</sup> for Allott et al. (2009), about 660 m<sup>2</sup> for Holden et al. (2006), and 2500 m<sup>2</sup> for

Luscombe et al. (2016), sampling methods were so different that their sampling density, defined as number of sampling points per unit area (m<sup>2</sup>) in percentage, was about 2.3%, 4%, and 15%, respectively. This means that in a watershed with an area of 0.1 km<sup>2</sup>, the equivalent sample size would be 2300, 4000, and 15,000 respectively. The huge samples are almost impossible to be obtained in reality and the discrepancy among them leaves a great uncertainty on how many WTD samples should be taken even in a 0.1-km<sup>2</sup> watershed.

Do natural gullies and artificial ditches have similar impacts on WTDs both laterally and longitudinally? Previous studies have not clearly addressed how WTDs would change when both types of channels are available within a peatland watershed.

The purpose of this study is to answer these questions by collecting WTD data in a small watershed within Zoige peatland, located in the northeastern Qinghai-Tibet Plateau of China. The Zoige peatland is a unique alpine peatland among all peatlands in the world (Xu et al., 2018). Yet, none of earlier studies on short-term peatland hydrological processes and water budget focused on this peatland. Thus, this study would fill the geographical gap in understanding hydrology of global peatlands. In addition to determining the trend of WTDs in the longitudinal direction of gullies and ditches for answering the third question, we also adopted two geostatistical methods, hotspot analysis and geographically weighted regression (GWR) (Anselin, 1995; Fotheringham et al., 2002; Lewandowska-Gwarda and Antczak, 2017), to examine spatial patterns of WTDs for answering the first two questions. The hotspot analysis is based on kriging interpolation, which has been used to build models for predicting spatial patterns of WTD (Desbarats et al., 2002; Lyon et al., 2006; Moore et al., 1991). GWR is also a classic method that has been widely used to explore spatial relationships among spatially related variables (Brown, 2017; Gutierrez-Posada et al., 2017; Kerry et al., 2017; Sheng et al., 2017; Tu, 2011).

In this study, we investigated spatial and temporal characteristics of WTDs in a small watershed located in a disturbed upland within the Zoige peatland of China. We first examined local spatial patterns of

measured WTDs,  $H$ , and  $S$  in the study watershed using the hotspot analysis. Then, we explored the spatial relationships between WTDs and  $H$  and  $S$  using the GWR model. Next, we measured and analyzed WTDs in the lateral and longitudinal directions of several gullies and ditches. At last, we answered the three questions based on the results.

## 2. Materials and methods

### 2.1. Study area

The Zoige basin was formed by the uplift of the Qinghai-Tibet Plateau and subsequently infilled by lacustrine sediment (Wang et al., 1995). With the elevation ranging between 3400 and 3900 m, it is now characterized by a relatively smooth surface generally inclining from southeast to northwest. The two local rivers (i.e., White and Black Rivers) flow along the same direction and converge into the first bend (U-shape) of the Upper Yellow River in China (Fig. 1a and b). The Zoige peatland developed within the basin about 10,000 years ago and expanded between 6000 and 3000 years ago (Zeng et al., 2017). The originally formed peats were mainly percolation mires, but gradually turned into surface-flow mires (Joosten and Schumann, 2007). In modern time, the peatland has experienced continuous degradation because of intensified human activities (Yang et al., 2017; Yu et al., 2017) and climate change. Although it currently only covers about 19% of the basin, the Zoige peatland is distributed around the entire basin with an area of approximately 3500 km<sup>2</sup> (Fig. 1b), forming the world largest high-altitude peatland (Joosten et al., 2008).

The study area was a small watershed located in an upslope peatland near the upstream end of the Black River, 32° 57' 46" N, 103° 00' 23" E (i.e., the red dot in Fig. 1b). It includes a fluvial valley bounded by mountains on the eastern, southern, and western sides with a total area of about 0.151 km<sup>2</sup>. Elevations are generally high on the south and low on the north sides and decrease from eastern and western sides to the valley (Fig. 1c). The main stream runs from the south end straightly to the north outlet. And many shallow and small artificial drain channels were created by nomad for grazing. Rainfall in the study area typically occurs during the monsoon season that lasts from the beginning of May to the end of September, accompanied with relatively high temperatures.

### 2.2. Field measurements

We measured elevations using a differential GPS (Trimble R2) with vertical and horizontal accuracies of  $\pm 0.85$  and  $\pm 0.50$  m respectively. And the digital terrain model created from these points provided a continuous representation of the study watershed with a mean resolution of 13 m. Peats were generally deep in and near the valley and shallow toward the east and west edges with relatively steep slopes. A total of 119 peat depths was measured across the study watershed using self-made augers with the length ranging between 1.5 and 2.5 m as shown in Fig. 2.

Water table depth (WTD) was measured at 114 locations carefully selected to cover topographic variations of the study watershed using conventional dipwells as shown in Fig. 2. Each dipwell, which was 110 cm long, was made of an iron tube with inner and outer diameters of 0.018 and 0.02 m respectively. WTDs in these locations were measured on the 17th (114 points), 20th (103 points), and 23th (105 points) of May, July 17th (77 points), and September 18th (81 points) respectively. The reduction of the measured WTD numbers in July and September was mainly caused by loss of dipwells due to vandalism from local residents. Sample locations were determined using a stratified random sampling method – that is selecting less number of samples sparsely over the relatively flat area, while more in the steep area.

A transect of dipwells was installed perpendicular to the downstream reach of the main stream and a shallow ditch, respectively. In the stream, the bed has already cut through the peat layer with a layer

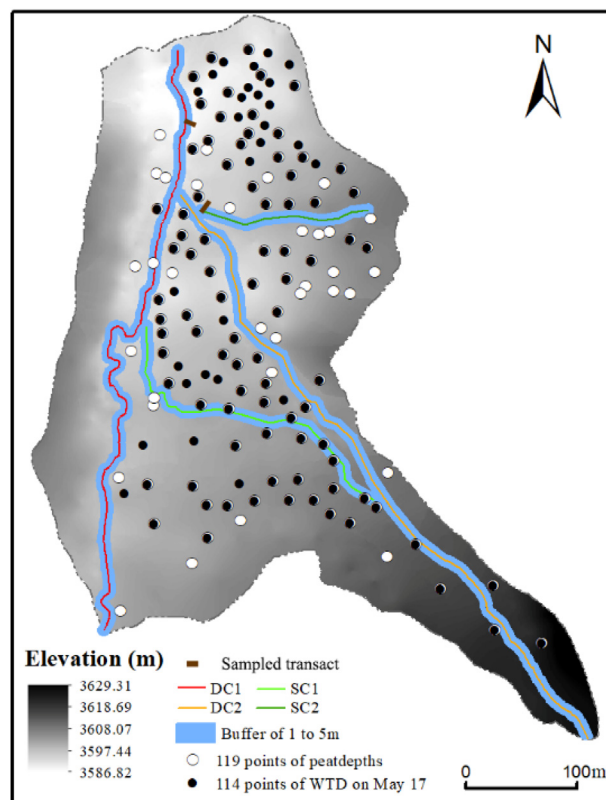


Fig. 2. Demonstration of the sampling design. The buffer zones were created for calculating mean WTDs along these gullies and ditches.

of mineral soil about 30 cm thick exposed. In the ditch, however, the bed was well within the peat layer. Each transect contained eight dipwells that were 1 m apart from each other. The nearest dipwell was about 2 m away from the edge of the stream and gully. WTDs were measured on several individual days between May and September 2017.

### 2.3. Data analysis

#### 2.3.1. Geostatistical analysis

The originally obtained discrete values of WTD,  $H$ , and  $S$  were first converted into continuous ones with the same number of Thiessen polygons (Bailey and Gatrell, 1995) using a kriging method selected from five different ones based on their geostatistical properties. Then, spatial variations of WTDs,  $H$ , and  $S$  were characterized by their localized spatial patterns, which may be statistically described by hot spots (areas with similar high values) and cold spots (areas with similar low values) (Mitchell, 2005). We then established GWR models (Fotheringham et al., 2000):

$$u_i = c_0(x_i, y_i) + c_1(x_i, y_i)v_{1i} + c_2(x_i, y_i)v_{2i} + \varepsilon_i \quad (1)$$

where  $u_i$  is the dependent variable representing in this study WTDs for a given measured day at one of the selected points,  $v_{1i}$  and  $v_{2i}$  are the first and second independent variables representing  $H$  and  $S$  at the same point respectively,  $c_0$ ,  $c_1$ , and  $c_2$  are coefficients that have different values at different locations  $(x_i, y_i)$ , and  $\varepsilon_i$  is the spatially variable residuals. The GWR model addresses spatial heterogeneity issues at a local scale by incorporating the spatial complexities resulting from variations in scale and location (Ahmed et al., 2017; Kim et al., 2017). Technically, a GWR model relies on local windows (or areas) identified in terms of the spatial heterogeneity of the data to determine local correlation coefficients for all independent variables. In this study, the GWR tool in ArcGIS was used to construct the GWR model for each

dependent variable (i.e., WTDs measured on each day). Preliminary tests revealed that the two options for the kernel function (i.e., FIXED and ADAPTIVE), which is adopted in ArcGIS to automatically generate the windows/areas, led to similar model results. Thus the first kernel function was used, which assured that each kernel (i.e., each local area) includes at least 45 points. The goodness-of-fit for each GWR model was evaluated using the value of the adjusted  $R^2$  for the overall model prediction, rather than  $R^2$ , to account for the impact of degree of freedom on  $R^2$ . The adjusted  $R^2$  may be obtained directly from the results of GWR modeling in ArcGIS.

Given that the calculated local coefficients for the two independent variables (i.e.,  $c_1$ , and  $c_2$ ) may not be always statistically significant, directly demonstrating the spatial distributions of these coefficients would not be useful. Accordingly, ArcGIS calculates the  $p$ -value for indicating the statistical significance of the coefficient at each local kernel (or area) using data points falling within it. We then reclassified these  $p$ -values into three classes,  $p > 0.1$ ,  $0.1 \geq p \geq -0.1$ ,  $p < -0.1$  in which the first and third classes represent local areas in which coefficients are statistically significant at the 90% confidence interval, while the second denotes the local areas where coefficients are not statistically significant. By comparing the spatial correlations between the areas of the two statistically significant coefficients, we examined the localized spatial relationships between each WTD dataset and the two relevant variables,  $H$  and  $S$ .

### 2.3.2. Impacts of ditches and gullies on WTDs

To facilitate the analysis, the gullies and ditches in the study watershed were generally divided into (i) deep gullies and (ii) shallow ditches (Fig. 2). The former were generally deep and have perennial flows, while the latter were typically shallow and tend to be dry not long after each rainfall event. Their impacts on WTD values were examined by quantifying WTD changes in the lateral (i.e., perpendicular to the channel) and longitudinal directions. The sampled transect next to the main stream and the shallow gully was denoted as transect 1 and 2 respectively (Fig. 2). Measured values of WTD in each transect on multiple days were plotted against the lateral distance to show their changes.

The analysis along the longitudinal direction started with selecting two from each type of the gully/ditch network existed in the study watershed. Two selected deeper gullies were termed deep channel (DC) 1 and 2, whereas two selected shallow ditches were referred to as shallow channel (SC) 1 and 2 (Fig. 2). Along each selected channel, a buffer zone ranging between 1 and 5 m from the channel was generated using each set of WTD data converted into a distributed raster GIS data with the resolution of 1 m. The significant water-table drawdown effect within the 1-m neighboring area of channels (Allott et al., 2009; Holden et al., 2006; Luscombe et al., 2016) may compromise the possible trends of the longitudinal WTDs and thus this area was excluded from the buffer zone. Within each buffer zone, the mean of WTDs in a small section of 3–5 m along the channel was calculated (Fig. 2) and subsequently plotted against the longitudinal distance.

## 3. Results and analysis

### 3.1. Localized spatial patterns of WTDs, $H$ and $S$

Hotspots for WTDs,  $H$ , and  $S$  (Fig. 3a–g) represented localized spatial patterns of the three variables with statistical significance. In May, hotspots stayed around the areas on the eastern and western edges where WTDs were high (Fig. 3a–c). The two main cold spots were also consistent with the concentrated areas of low WTDs. Similar localized spatial patterns existed in the wet September (Fig. 3e). In the dry July (Fig. 3d), distributions of hot and cold spots were partially different from those in May and September, indicating that localized high and low WTD areas shifted in July. Similarly, the hot and cold spots of  $H$  and  $S$  verified existence of localized spatial patterns with statistical

significance for  $H$  and  $S$  (Fig. 3f, g).

The cold spots of the three WTD datasets in May shared a similar distribution. Although hotspots of WTDs on May 17 were partially different from those in the other two days of May, their spatial distributions were similar (Fig. 3a–c). These features suggested that under the similar rainfall condition of May, the spatial pattern of WTDs did not change with time significantly. In the wet September (Fig. 3e), WTDs had a very similar localized spatial pattern to those in May. Yet, in the dry July, one of the main hotspot clusters moved up to the southeastern corner of the watershed, while the area of the cold-spot cluster on the south was reduced significantly (Fig. 3d). This difference among the three months suggested that during the summer (i.e., from May to September), the spatial pattern of WTDs could be significantly different between the wet period when rainfall frequency is high and dry period when little or no rainfall occurs.

### 3.2. Spatial correlation between WTDs and $H$ and $S$

GWR modeling analysis using WTDs for each of the five sampling days showed that the established GWR models had (adjusted)  $R^2$ , which considered the impact of the number of independent variables on the results, ranged between 0.828 and 0.918, apparently suggesting that predicted WTDs could overall explain a large part of changes in the measured WTDs. The mean value of the intercept (i.e.,  $c_0$  in Eq. (1)) in the established GWR was 25.0, 24.2, 20.6, 38.6, and 10.1 cm for 5/17, 5/20, 5/23, 7/17, and 9/18 respectively. These values indicated that water table was generally high in September, low in July, and medium in May, which was consistent with the associated weather conditions.

Coefficients  $c_1$ , and  $c_2$ , which represent the influence of  $H$  and  $S$  on WTDs, varied spatially (Fig. 4). On 5/17/2017, peat depths in about 45% of the total area were significantly correlated with the associated WTDs, among which about 15% (i.e., within  $p \leq -0.1$ ) and 30% (i.e., within  $p \geq 0.1$ ) had negative and positive correlation respectively (Table 1). These two types of areas were mixed together and did not display specific spatial patterns (Fig. 4). In the remaining four data sets, the area that had statistically significant correlation took between 51% and 57% of the total area. Majority of this area had negative correlation (46–47%) and only < 11% of the area had positive correlation (Table 1). The negative correlation means that the deeper the peat depth is, the smaller the WTD (i.e. the higher the groundwater level) is. In late May, the area with negative correlation dominated the northern and middle parts of the watershed, while in July and September, it extended to the southern part (Fig. 4).

Slope gradients showed different correlation patterns (i.e.,  $c_2$ ). For all WTD data sets, the areas with statistical significance took only about 16% to 23% of the total area (Table 1). The proportions of the negative and positive correlations within the limited areas varied wildly among the five data sets. The former was less than the latter for the 5/17/2017, 5/20/2017, and 7/17/2017 data sets, while the opposite held for the remaining two data sets (Table 1). Apparently, slope had a very limited influence on WTD values.

The area with no statistical significance for  $H$  ranged between 44 and 55%, while for  $S$  varied from 77 to 85% (Table 1 and Fig. 4) suggesting that in these areas, values of  $H$  and  $S$  were insufficient to explain spatial variations of WTDs. Therefore, neither localized spatial pattern of  $H$  nor  $S$  could explain that of WTDs. The nature of localized spatial correlations between WTDs and  $H$  and  $S$  further signified the complexity of spatial and temporal patterns of WTD.

### 3.3. Variations of WTDs in the lateral direction of gullies and ditches

Along the transect next to the main stream (i.e., transect 1), trends of WTDs varied among the three months (Fig. 5a). In the relatively wet May, WTDs on 5/17/2017 were generally low. The WTD value increased sharply from  $-74$  to  $-27$  cm within the distance from 2 to 5 m away from the channel edge. In the rest 3 m, it remained similar with

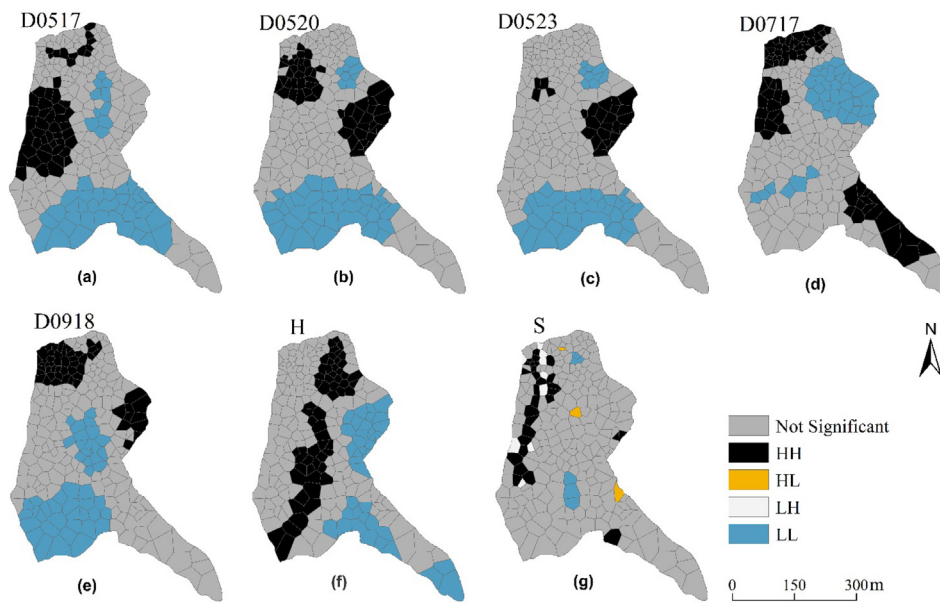


**Fig. 3.** Localized spatial clusters of the measured WTDs on the five measurement days (a)–(e), *H* (f), and *S* (g) in the study watershed. HH – hotspots (areas with similar high values), LL – cold spots (areas with similar high values), HL and LH – spots (areas mixed with low and high WTD, *H*, or *S* values).

local variations. On the other two days (Fig. 5a), WTD values were relatively similar to those on 5/17/2017, smaller in the distance between 2 and 4 m away from the edge and greater in the remaining distance. Considering WTD values in all three days, variation of WTD values at the location closer to the edge was the highest, suggesting the high variability of WTDs at this location. In the dry July, the WTDs on the three consecutive days showed similar patterns of changes except that on 7/18/2017, the WTD value was higher than those of the two other days at the location 8 m away from the channel edge. In the wet September, the WTD value at the closest location to the edge (–33.5 cm) was higher than that at its nearest neighbor (–40 cm) (Fig. 5a).

Although these WTD trends varied greatly among the three months, they showed a general increasing trend in the lateral direction.

Regression analysis showed that WTDs in each month may be fitted well by a linear model because the two coefficients (*a* and *b*) and  $R^2$  were all statistically significant (Table 2). The slope of the linear model was the highest in May (6.720) and lowest in July (3.277), indicating that the drawdown effect on water table caused by the stream was high in May and low in July. Higher precipitation in September apparently offset to some degree the drawdown effect.

Trends of WTDs along transect 2 were different (Fig. 5b). In May, the two WTD sets followed a similar trend: low at the location 2 m away from the edge of the gully and then stayed almost the same in the remaining distance with minor local variations. In July, they were significantly different from one another, though their trends were similar. The WTD values on 7/18/2017 were indeed close to those on 5/23/2017 at all locations except the first one where it was even higher than

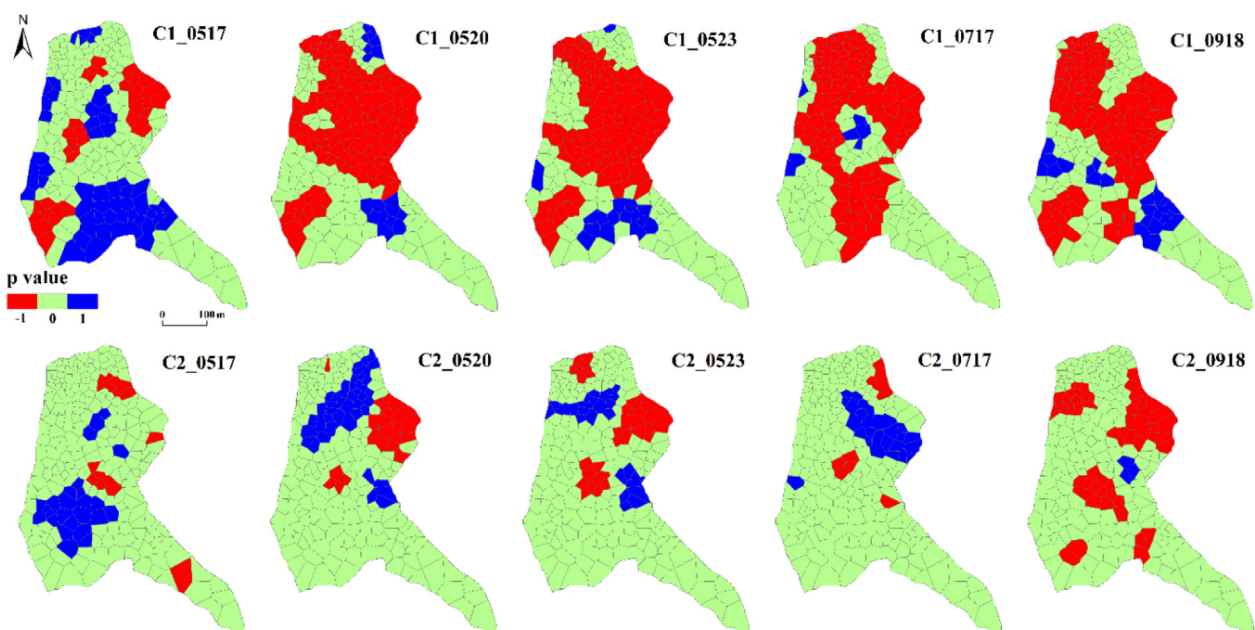


**Fig. 4.** Results of GWR modeling.  $c_1$  and  $c_2$  were two spatially variable coefficients reflecting the local correlation between WTDs and *H* and *S* respectively. These maps actually showed the statistical significance of  $c_1$  and  $c_2$ , rather than their values.

**Table 1**  
Proportions of areas with negative, no, and positive correlations.

Data set	$c_1$ (for H)			$c_2$ (for S)		
	$p \leq -0.1$	$-0.1 < p < 0.1$	$p \geq 0.1$	$p \leq -0.1$	$-0.1 < p < 0.1$	$p \geq 0.1$
5/17	15.27	54.86	29.87	6.24	80.54	13.23
5/20	47.03	46.59	6.38	9.12	77.45	13.43
5/23	46.54	44.69	8.76	11.27	80.57	8.16
7/17	47.11	49.80	3.09	4.11	85.45	10.44
9/18	45.77	43.95	10.28	22.05	76.66	1.29

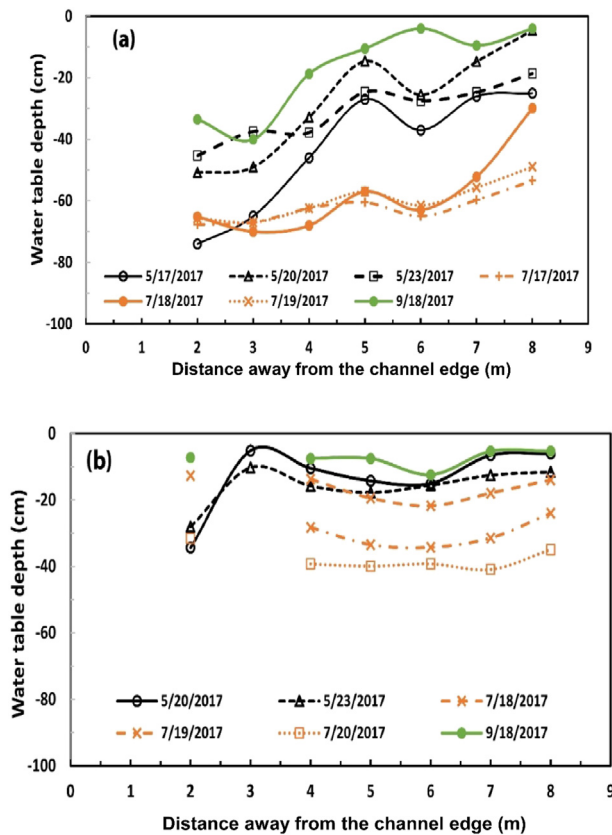


**Fig. 5.** Changes of WTDs along the two transects in the lateral direction of a (a) deep and (b) shallow channel. Note: the origin in both (a) and (b) represented the edge of the deep and shallow channel where the lateral transect starts.

**Table 2**  
Linear regression models for WTDs along transect 1.

Month	$a$	$b$	$R^2$	$p$ -value
May	6.720	-67.315	0.878	< 0.01*
July	3.277	-76.349	0.743	< 0.01*
September	5.865	-46.493	0.776	< 0.01*

\* This value means that the  $p$ -values for  $a$ ,  $b$ , and  $R^2$  are all < 0.01.

that on 5/23/2017 (Fig. 5b). In September, the WTDs were also very similar to those in May except that it was higher at the location 2 m away from the edge of the gully. Overall, WTD trends in all measured days were more similar than discrepant. Although some trends showed an increasing tendency (e.g., those on 7/19/2017 and 7/20/2017), regression analysis indicated that their linear models were not statistically significant, suggesting that WTD values did not change significantly along the lateral transects, regardless of precipitation.

**3.4. Variations of WTDs in the longitudinal direction of gullies and ditches**

In May, three longitudinal trends (Fig. 6a) were ostensibly different. Mean WTD values on 05/17 decreased gently in the first 100 m and then continuously decreased with a much faster rate till about 320 m downstream. It continuously increased with a similar rate and accelerated from about 570 m to the end where the WTD value lower than that at the beginning (Fig. 6a). The three abrupt changes of the local trends occurred at the conjunctions with gullies. On the other two days in May, mean WTDs decreased continuously with a similar trend till the location about 480 m downstream where a gully merged into it. The two locations where the trends changed locally in the remaining stream section were apparently consistent with the convergence of two gullies. Impact of tributary gullies along the main stream on WTDs at the junctions seemed varying both spatially and temporally. In July, mean WTDs were generally lower with a higher degree of variation, while in September, they were higher with a lower degree of variation (Fig. 6a). Despite of these local variations, mean WTDs generally decreased in all three months. The decrease followed a statistically significant linear trend with the highest rate in May and the lowest in September (Table 3).

Although mean WTDs on each sampling day linearly decreased along the stream segment, these linear trends could not be collapsed to a single one again suggesting their strong temporal variation. Along the same stream segment (i.e., DC1), peat depth varied greatly in the first 200 m and then became less changed between 200 and 360 m, which was followed by an oscillated pattern in the remaining distance. Overall, it did not show clear correlation with the changes of mean WTDs in any month.

Along a long gully (i.e., DC2), patterns of mean WTDs were still variable (Fig. 6b). Trends on the three days in May were similar with those on 05/17 generally lower than those on the other two. At the junction points to the two small gullies about 250 and 540 m downstream of DC2, local increases of the mean WTDs occurred on all three days and then began to decrease. In both July and September, mean WTDs remained roughly unchanged even passing the first conjunction point at around 250 m downstream (Fig. 6b) and started to increase at the location about 400 m downstream. Then, the change of the mean WTDs in September only happened once at around 550 m downstream but in July occurred twice before and after this location. Again, impact of gullies on the mean WTDs at the junctions was temporally variable, reflecting complexity of the WTD distribution.

Compared with those along DC1, trends in the three months along DC2 were not consistent with one another. The WTDs in May followed a linearly decreased trend, while those in July and September showed a linearly increasing trend (Table 3). Rates of changes along DC2 were generally less than those along DC1, though DC2 had a similar length to DC1. Again, mean WTDs along DC2 were generally low in September and high in July, which were consistent with the rainfall pattern in these months. The peat depths generally increased along DC2 with the rate of changes varied greatly at the local scale (Fig. 6b). Still, there was no clear correlation between peat depths and mean WTDs. Clearly, even within the same type of deep channels (i.e., DC1 and DC2), the downslope changes of WTDs were diverse.

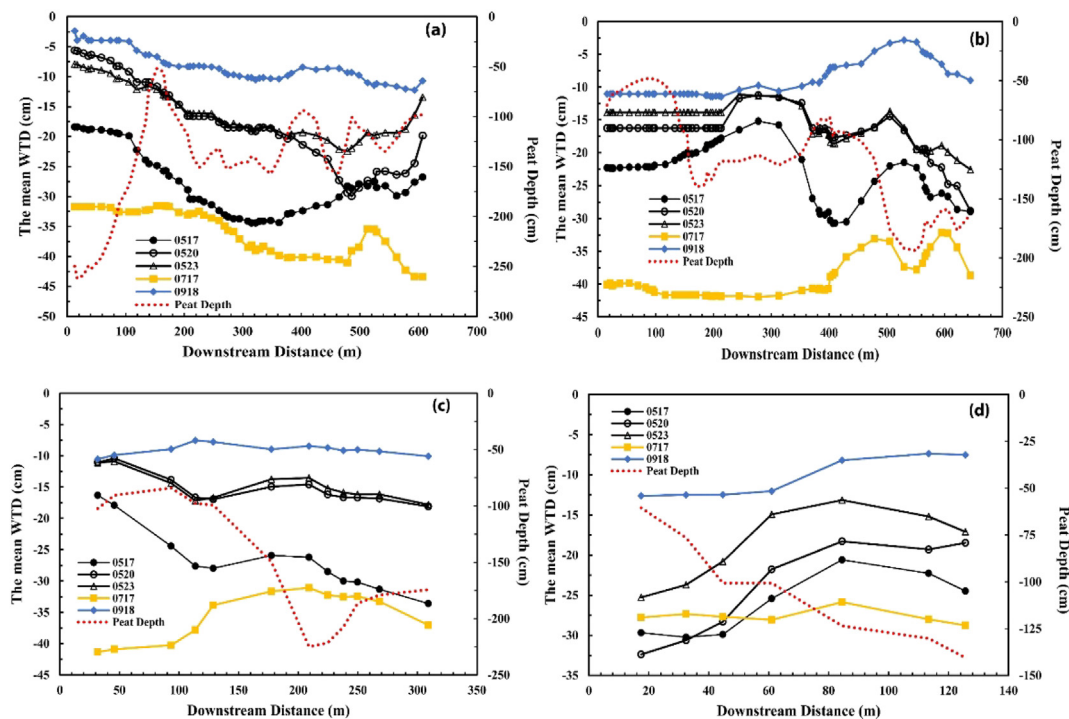


Fig. 6. Changes of WTDs in the longitudinal direction of (a) DC1, (b) DC2, (c) SC1, and (d) SC2. The red dashed curve represented the associated changes of peat depths. (For interpretation of the references to colour in this figure legend, the reader is referred to the web version of this article.)

Table 3  
Linear regression models for WTDs along the four different streams and gullies.

Selected channel	Month	$\alpha$	$b$	$R^2$	$p$ -value
DC1	May	-0.0257	-12.992	0.745	< 0.01*
	July	-0.0187	-30.398	0.743	< 0.01
	September	-0.0133	-4.407	0.780	< 0.01
DC2	May	-0.0108	-15.408	0.486	< 0.01
	July	0.0111	-42.640	0.548	< 0.01
	September	0.0113	-12.376	0.699	< 0.01
SC1	May	-0.0298	-13.728	0.707	< 0.01
	July	0.0304	-40.654	0.506	< 0.01
	September	0.0004	-9.079	0.0015	> 0.05**
SC2	May	0.0998	-29.773	0.7266	< 0.01
	July	0.0584	-14.386	0.893	< 0.01
	September	-0.0051	-27.285	0.054	> 0.05

\* This value means that the  $p$ -values for  $\alpha$ ,  $b$ , and  $R^2$  are all < 0.01.  
 \*\* This value means that the  $p$ -value for  $R^2$  is > 0.05 and the model is not statistically significant.

Mean WTDs along SC1 and SC2 displayed distinct characteristics. The trend of mean WTDs along SC1 on 05/17 was significantly different from those on 05/20 and 05/23, which were almost identical (Fig. 6c), again indicating the great temporal variation in May. Two discernable local changes occurred at the locations about 120 and 210 m downstream of SC1. These changes were persistent in July when mean WTDs were relatively low, but diminishing in September when they were generally high. At the beginning of SC1, mean WTDs in late May were similar to those in September, which was not the case in DC1 and DC2, though those in July were still the lowest (Fig. 6a–c). In May, mean WTDs globally decreased linearly, but in July they increased linearly with a higher rate (Table 3). In September, mean WTDs almost remained the same along the ditch. Mean WTDs were generally high in September, medium in July, and low in May (Fig. 6c), suggesting that they were controlled by different rainfall patterns in these months. Peat depths along SC1 varied greatly, yet, was inconsistent with that of mean WTDs (Fig. 6c), suggesting that changes of mean WTDs along SC1 was

not correlated with that of the peat depths either.

Values of mean WTDs along SC2 were discernably different on the three days in May with a local change at the location about 60 m downstream of the ditch (Fig. 6d). A similar change existed in July and September. Nonetheless, in the beginning section of SC2, mean WTDs in July were higher than those on 05/17 and 05/20, though those in September were still the highest. This local characteristic was different from that in all other three channels. The three trends of mean WTDs along SC2 in May were similar and may be described by a statistically significant linear function with a positive increasing rate (Table 3). Values of mean WTDs in July did not change obviously and their trend in September followed a clear linear pattern with a positive rate. Temporal variation of all trends in these three months was much less than that along DC1, DC2, and SC1. The peat depth along SC2 increased almost linearly (Fig. 6d), which was apparently at odds with the trends of mean WTDs in all three months. This again suggested that the variation of WTDs was not clearly affected by the associated peat depth.

#### 4. Discussion

##### 4.1. Spatially variable WTDs at the watershed scale

While our data were only from one year (2017), they covered the most dynamic period of annual WTDs. Thus they reflected the possible range of WTD variations in the Zoige peatland. Spatial distribution of the measured WTDs demonstrated highly localized clusters with signs of temporal changes (Fig. 3). Therefore, the variable spatial pattern of WTDs is hard to quantify. Furthermore, peat depth may appropriately explain changes of WTDs (i.e., the deeper the depth, the smaller the WTD value) in < 48% of the total area, whereas the area where slope gradients correctly explained the WTD variation only took no > 14% of the total (Table 1). Therefore, changes of  $H$  and  $S$  fail to account for WTD variations in the study watershed, which explains why the spatially variable WTDs in the Peak District peatland, UK cannot be well characterized using the wetness index, which is a function of  $S$  (Figs. 17 and 18 in Allott et al. (2009)). It also suggests that at the watershed

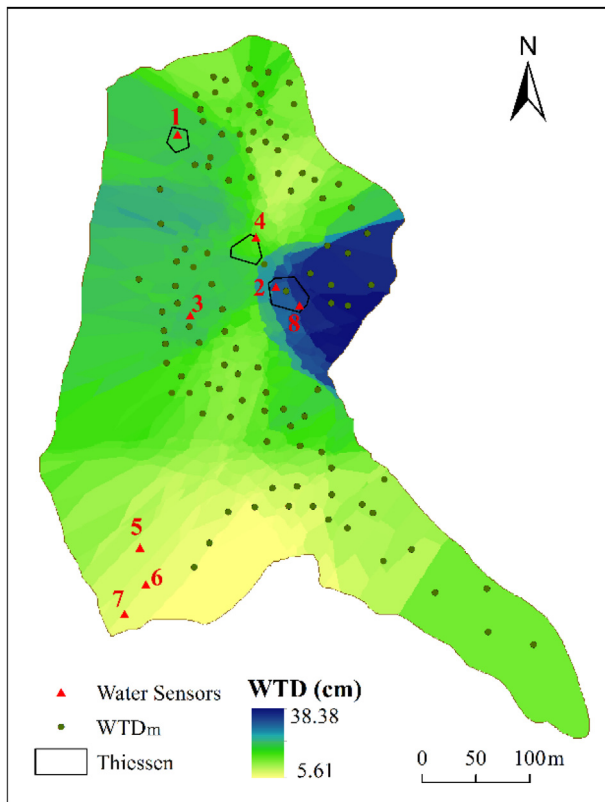


**Fig. 7.** Locations of the eight water sensors installed in the study watershed and the associated Thiessen polygons.  $WTD_m$  represents the data measured using dipwells on 5/23/2017,  $WTD$  (cm) is the distributed  $WTD$  values calculated using the originally measured  $WTD_m$ . Thiessen polygons were described in the methods section.

scale, the spatial distribution of  $WTD$ s cannot be described by simply measuring  $H$  and  $S$  and establishing a relationship between them. Although new sampling methods such as using Unmanned Aerial Vehicles (UAV) have been developed (Rahman et al., 2017), they were only limited to very wet conditions with more saturated areas. Obviously, the most reliable means of determining spatial variation of  $WTD$ s is still *in situ* sampling (Luscombe et al., 2016).

#### 4.2. Hydrologically significant sampling strategy

Our sampling design, which selects variable numbers of samples based on topographic changes, greatly reduced sampling densities (0.05–0.075%), while may cover spatially variable  $WTD$ s. To understand its reliability, we measured temporally continuous  $WTD$  values using eight water sensors at eight different locations within the study watershed and compared these  $WTD$  values with those extracted from the spatial distribution of  $WTD$ s on 5/23/2017 (Fig. 7). At three locations (i.e., No. 1, 4, and 8), the  $WTD$  values obtained using two independent methods were significantly different, though they were similar in other five locations (Fig. 8), suggesting that our sampling method and the subsequent interpolation analysis could not guaranty that calculated  $WTD$ s are always accurate. Nonetheless, two-sample difference test showed that the two  $WTD$  sets were not statistically different, meaning that relatively larger errors in some individual locations would not affect the statistical properties of  $WTD$ s (e.g., mean, or spatial pattern) over the entire study watershed. For example, in the Thiessen polygons that include three water sensors (i.e., No. 1, 4, and 8) (Fig. 7), the relatively larger errors would only lead to  $< 0.1\%$  of error in calculating the mean  $WTD$  of each Thiessen.

Thus, our sampling strategy is reasonable for characterizing spatial

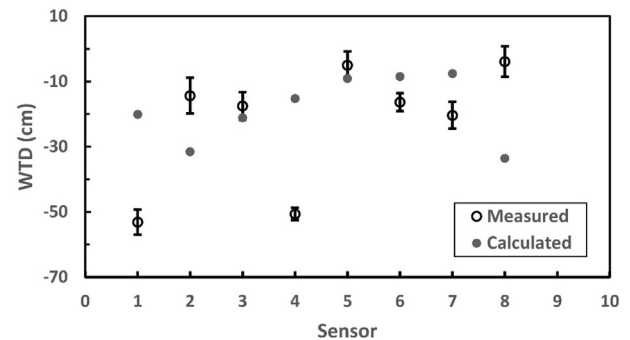


**Fig. 8.** Comparison of  $WTD$ s at the eight locations on 5/23/2017. The solid dots were  $WTD$  values extracted from the interpolated distribution of  $WTD$ s based on the 105 points obtained on 5/23/2017 from the study watershed. The open circles were the means of continuous  $WTD$  values measured with a 15-minute interval by water sensors on the same day and the associated vertical bars were standard deviations of these continuous  $WTD$ s.

distributions of  $WTD$ s at the watershed scale. Hydrologically, the obtained spatially distributed  $WTD$ s entail assessing temporal changes of peatland storage water. In our case, from May to July, about  $1406 \text{ m}^3$  of the stored water moved out of the peatland, whereas from July to September and from May to September, about  $2309$  and  $903 \text{ m}^3$  of the stored water was gained from rainfall in the study watershed respectively. This pattern is consistent with the mean daily precipitation associated with these three periods, which were 2.40, 4.15, and  $3.27 \text{ mm}$  respectively.

#### 4.3. Impact of ditches and gullies on $WTD$ s

Our analyses showed that in the lateral direction of gullies and ditches,  $WTD$ s had obvious temporal variations during summer, 2017. In the distance near the channel edge (i.e.,  $< 4 \text{ m}$  away from the edge) (Fig. 9a),  $WTD$ s in transect 1 were noticeably higher than those in transect 2, indicating that a deeper channel had greater impact on  $WTD$ s. In the distance 4–8 m away from the channel edge,  $WTD$ s in transect 1 were even lower than those in transect 2, signifying that water table retrieved back to a higher level in transect 1 than in transect 2. Along the entire transect 1, the  $WTD$  was high at the beginning and continuously decreased till the end that was 8 m away from the edge. Yet, along the entire transect 2,  $WTD$ s were generally high except that at the location 3 m away from the edge (Fig. 9a). These two patterns revealed three findings. First, deep channels had greater impact on water table in the neighboring peats, giving rise to the well-known distance decay effect (Allott et al., 2009; Holden et al., 2006; Holden et al., 2011; Luscombe et al., 2016). The effect diminished around the distance about 4 m away from the channel edge. Second, shallow ditches generally had no discernable influence on water table in the nearby peats. Third, in the area not immediately next, but still close to the edge (i.e., the zone about 4–8 m away from the edge),  $WTD$ s were more controlled by other factors such as peat depth, slope, and peat physical properties, which might explain the fact that water table was higher in this zone for transect 1 than that for transect 2 (Fig. 9a).

For the two deep channels (i.e., DC1 and DC2),  $WTD$ s increased downslope along DC1 and then remained roughly constant with a decreasing trend close to the end, whereas  $WTD$ s stayed the same downslope along DC2 and then oscillated around the mean with a local increasing trend toward the end (Fig. 9b). These different trends suggested that changes of  $WTD$ s along deeper channels were diverse, though there was a weak tendency that  $WTD$ s tended to be higher in the downslope sections of the channels. Changes of  $WTD$ s along the two shallow channels (i.e., SC1 and SC2) were even more diverse (Fig. 9b). SC1 was longer than SC2, but  $WTD$ s along SC1 were much less variable than those along SC2. The sharp decrease and then increase of  $WTD$ s

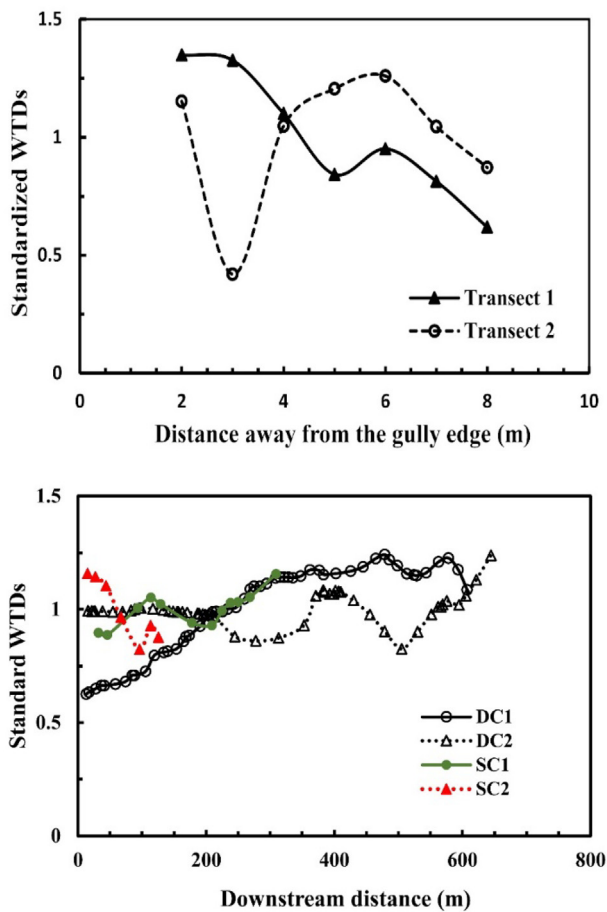


Fig. 9. Changes of the standardized WTDs in the (a) two transects in the lateral direction of the channels, and (b) four selected channels in the longitudinal direction.

along SC2 might not be due to the presence of SC2 because SC2 had the shortest length among the four channels. Overall, downslope changes of WTDs along the two types of channels were not significantly different. Given that most previous studies only focused on the lateral impact of ditches and gullies on peatland hydrology (Allott et al., 2009; Holden et al., 2006; Holden et al., 2011; Luscombe et al., 2016), our analyses provided new insight into how ditches and gullies change peat hydrology.

## 5. Conclusions

Spatial and temporal variations of water table depth (WTD) in peats are so complex that their patterns at the watershed scale have not been fully studied. We investigated this issue by measuring spatially distributed WTDs, peat depths ( $H$ ), and slope gradients ( $S$ ) in a small watershed of about 0.151 km<sup>2</sup> in the Zoige basin of the Qinghai-Tibet Plateau, China in the summer (May–September) of 2017. Our analyses allowed us to answer the three questions raised earlier:

- (1) In the study watershed, spatial distributions of WTDs showed strong localized clusters, which also changed with time. There is no single spatial pattern that may be used to characterize spatial distributions of WTDs at different times. Also, spatially distributed WTDs cannot be predicted using spatially variable  $H$  and  $S$  values in the study watershed. Given that the study watershed has a typical physical setting in the Zoige basin, this finding should be applicable to the entire basin.
- (2) Although limited individual samples with the sampling density of as

low as 0.05% were collected using our stratified random sampling method, they may be used to obtain spatial distributions of WTDs in the study watershed. These spatially distributed WTDs provide valuable information for establishing water budget at the watershed scale. As the peatland area increases, this sampling method, which took less samples in the relatively flat area, while more samples in the relatively steep area, will be more useful and thus should be adopted in the future for sampling large-scale WTDs.

- (3) Deeper gullies whose beds typically cut through the peat layer can cause the drawdown effect of WTDs in the lateral direction within a 4-m adjacent peat zone. Shallow ones with their beds remaining in the peat layer do not affect WTDs significantly. The longitudinal changes of WTDs along any types of gullies or ditches did not have any statistically significant trend. It is important to distinguish deep gullies from shallow ditches based on whether their beds cut through the peat layer or not because peats next to them have different hydrological responses. Future peat restoration should mainly focus on managing deep gullies and ditches.

Our results indicated that the spatial and temporal variability of WTDs even within one summer of a year may be so complex that it could not be described by a simple spatial pattern. Thus, findings derived from and the sampling strategy developed in this study can be valuable knowledge for further understanding WTD variability over multiple years and the entire Zoige basin, as well as peatland watersheds in other regions.

## Declaration of Competing Interest

The authors declare that they have no known competing financial interests or personal relationships that could have appeared to influence the work reported in this paper.

## Acknowledgments

This study was supported by the National Natural Science Foundation of China, China (91647204, 51709020, 91547112), Open Project of State Key Laboratory of Plateau Ecology and Agriculture, Qinghai University, China (2017-KF-01), Project of Qinghai Science & Technology Department, China (2016-ZJ-Y01, 2017-HZ-802), Open Research Fund Program of State key Laboratory of Hydroscience and Engineering (sklhse-2019-A-03), and Oversea Expertise Introduction Project for Discipline Innovation, China (D18013). We would like to thank Professor Xuyue Hu for his support. We also thank Jing Liu, Yezhou Wu, Xu Yan, Xiang Li, Kaiyu Li, and Youyong Li for field assistance and Yuchi You for helping performing some data analysis and preparing some figures.

## Appendix A. Supplementary data

Supplementary data to this article can be found online at <https://doi.org/10.1016/j.jher.2020.01.004>.

## References

- Ahmed, M.A.A., Abd-Elrahman, A., Escobedo, F.J., Cropper, W.P., Martin, T.A., Timilsina, N., 2017. Spatially-explicit modeling of multi-scale drivers of aboveground forest biomass and water yield in watersheds of the Southeastern United States. *J. Environ. Manage.* 199, 158–171.
- Allott, T.E.H., Evans, M.G., Lindsay, J.B., Agnew, C.T., Freer, J.E., Jones, A., Parnell, M., 2009. Water tables in Peak District blanket peatlands. *Moors for the Future Report No. 17.* funded by the Environment Agency and National Trust. Hydrological benefits of moorland restoration., p. 49.
- Anselin, L., 1995. Local indicators of spatial association—LISA. *Geograph. Anal.* 27, 93–114.
- Bailey, T., Gatrell, A.C. (1995). *Interactive spatial data analysis*, by Prentice Hall, Malaysia, PA.
- Boelter, D.H., 1972. Water table drawdown around an open ditch in organic soils. *J. Hydrol.* 15, 329–340.

- Brown, I., 2017. Hierarchical bioclimate zonation to reference climate change across scales and its implications for nature conservation planning. *Appl. Geogr.* 85, 126–138.
- Carlson, K.M., Goodman, L.K., May-Tobin, C.C., 2015. Modeling relationships between water table depth and peat soil carbon loss in Southeast Asian plantations. *Environ. Res. Lett.* 10.
- Clymo, R.S., 2004. Hydraulic conductivity of peat at Ellergower Moss, Scotland. *Hydrol. Process.* 18, 261–274.
- Daniels, S.M., Agnew, C.T., Allott, T.E.H., Evans, M.G., 2008. Water table variability and runoff generation in an eroded peatland, South Pennines, UK. *J. Hydrol.* 361, 214–226.
- Desbarats, A.J., Logan, C.E., Hinton, M.J., Sharpe, D.R., 2002. On the kriging of water table elevations using collateral information from a digital elevation model. *J. Hydrol.* 255, 25–38.
- Evans, M.G., Burt, T.P., Holden, J., Adamson, J.K., 1999. Runoff generation and water table fluctuations in blanket peat: evidence from UK data spanning the dry summer of 1995. *J. Hydrol.* 221, 141–160.
- Fotheringham, A.S., Brunsdon, C., Charlton, M., 2000. *Quantitative Geography - perspectives on Spatial Data Analysis*. SAGE Publication, London, UK.
- Fotheringham, S.A., Brunsdon, C., Charlton, M., 2002. *Geographically Weighted Regression: The Analysis of Spatially Varying Relationships*. Wiley, Chichester, UK.
- Glaser, P.H., Wheeler, G.A., Gorham, E., Wright, H.E., 1981. The patterned mires of the red lake peatland, northern Minnesota - vegetation, water chemistry and landforms. *J. Ecol.* 69, 575–599.
- Gutiérrez-Posada, D., Rubiera-Morollón, F., Vinueza, A., 2017. Heterogeneity in the determinants of population growth at the local level: analysis of the Spanish case with a GWR approach. *Int. Reg. Sci. Rev.* 40, 211–240.
- Holden, J., Burt, T.P., 2002. Piping and pipeflow in a deep peat catchment. *Catena* 48, 163–199.
- Holden, J., Burt, T.P., 2003a. Hydrological studies on blanket peat: the significance of the acrotelm-catotelm model. *J. Ecol.* 91, 86–102.
- Holden, J., Burt, T.P., 2003b. Runoff production in blanket peat covered catchments. *Water Resour. Res.* 39, 1191–1202. doi:10.1029/2003WR002067.
- Holden, J., Chapman, P.J., Labadz, J.C., 2004. Artificial drainage of peatlands: hydrological and hydrochemical process and wetland restoration. *Prog. Phys. Geogr.* 28, 95–123.
- Holden, J., Evans, M.G., Burt, T.P., Horton, M., 2006. Impact of land drainage on peatland hydrology. *J. Environ. Qual.* 35, 1764–1778.
- Holden, J., Wallage, Z.E., Lane, S.N., McDonald, A.T., 2011. Water table dynamics in undisturbed, drained and restored blanket peat. *J. Hydrol.* 402, 103–114.
- Joosten, H., Haberl, A., Schumann, M., 2008. Degradation and restoration of peatlands on the Tibet Plateau. *PEATLANDS Int.* 1, 31–35.
- Joosten, H., Schumann, M., 2007. Hydrogenetic aspects of peatland restoration in Tibet and Kalimantan. *Global Environ. Res.* 11, 195–204.
- Kerry, R., Goovaerts, P., Gimenez, D., Oudemans, P.V., 2017. Investigating temporal and spatial patterns of cranberry yield in New Jersey fields. *Precis. Agric.* 18, 507–524.
- Kim, O.S., Nugent, J.B., Yi, Z.F., Newell, J.P., Curtis, A.J. (2017). A Mixed Application of Geographically Weighted Regression and Unsupervised Classification for Analyzing Latex Yield Variability in Yunnan, China. *Forests*, 8.
- Labadz, J., Allott, T., Evans, M., Butcher, D., Billett, M., Stainer, S., Yallop, A., Jones, P., Innerdale, M., Harmon, N., Maher, K., Bradbury, R., Mount, D., O'Brien, H., Hart, R., 2010. *Peatland Hydrology. Draft Scientific Review, commissioned by the IUCN UK Peatland Programme's Commission of Inquiry on Peatlands*, p. 52.
- Lewandowska-Gwarda, K., Antczak, E., 2017. What determines the permanent emigration of poles? The analysis of the spatial diversification of causes in three economic age groups. *Acta Oecon.* 67, 149–172.
- Lou, X.D., Zhai, S.Q., Kang, B., Hu, Y.L., Hu, L.L., 2014. Rapid response of hydrological loss of DOC to water table drawdown and warming in zoige peatland: results from a mesocosm Experiment. *PLoS One* 9.
- Luscombe, D.J., Anderson, K., Grand-Clement, E., Gatis, N., Ashe, J., Benaud, P., Smith, D., Brazier, R.E., 2016. How does drainage alter the hydrology of shallow degraded peatlands across multiple spatial scales? *J. Hydrol.* 541, 1329–1339.
- Lyon, S.W., Seibert, J., Lembo, A.J., Walter, M.T., Steenhuis, T.S., 2006. Geostatistical investigation into the temporal evolution of spatial structure in a shallow water table. *Hydrol. Earth Syst. Sci.* 10, 113–125.
- McCarter, C.P.R., Price, J.S., 2013. The hydrology of the Bois-des-Bel bog peatland restoration: 10 years post-restoration. *Ecol. Eng.* 55, 73–81.
- Mitchell, A., 2005. *The ESRI Guide to GIS Analysis Vol. 2 Spatial measurements & statistics*, ESRI Press, Redlands, California.
- Moore, I.D., Grayson, R.B., Ladson, A.R., 1991. Digital terrain modeling – a review of hydrological, geomorphological, and biological applications. *Hydrol. Process.* 5, 3–30.
- Prat-Guitart, N., Belcher, C.M., Thompson, D.K., Burns, P., Yearsley, J.M., 2017. Fine-scale distribution of moisture in the surface of a degraded blanket bog and its effects on the potential spread of smouldering fire. *Ecohydrology* 10.
- Price, J.S., Heathwaite, A.L., Baird, A.J., 2003. Hydrological processes in abandoned and restored peatlands: an overview of management approaches. *Wetlands Ecol. Manage.* 11, 65–83.
- Rahman, M.M., McDermid, G.J., Strack, M., Lovitt, J., 2017. A new method to map groundwater table in peatlands using unmanned aerial vehicles. *Remote Sens.* 9.
- Ramchunder, S.J., Brown, L.E., Holden, J., 2009. Environmental effects of drainage, drain-blocking and prescribed vegetation burning in UK upland peatlands. *Prog. Phys. Geogr.* 33, 49–79.
- Sheng, J.C., Han, X., Zhou, H., 2017. Spatially varying patterns of afforestation/reforestation and socio-economic factors in China: a geographically weighted regression approach. *J. Cleaner Prod.* 153, 362–371.
- Shi, X., Thornton, P.E., Ricciuto, D.M., Hanson, P.J., Mao, J., Sebestyen, S.D., Griffiths, N.A., Bisht, G., 2015. Representing northern peatland microtopography and hydrology within the Community Land Model. *Biogeosciences* 12, 6463–6477.
- Sikstrom, U., Hokka, H., 2016. Interactions between soil water conditions and forest stands in boreal forests with implications for ditch network maintenance. *Silva Fennica* 50, 1416.
- Smiljanic, M., Seo, J.W., Laadnelaid, A., van der Maaten-Theunissen, M., Stajic, B., Wilmsing, M., 2014. Peatland pines as a proxy for water table fluctuations: disentangling tree growth, hydrology and possible human influence. *Sci. Total Environ.* 500, 52–63.
- Tu, J., 2011. Spatially varying relationships between land use and water quality across an urbanization gradient explored by geographically weighted regression. *Appl. Geogr.* 31, 376–392.
- Van Seters, T.E., Price, J.S., 2001. The impact of peat harvesting and natural regeneration on the water balance of an abandoned cutover bog, Quebec. *Hydrol. Process.* 15, 233–248.
- Wallage, Z.E., Holden, J., 2011. Near-surface macropore flow and saturated hydraulic conductivity in drained and restored blanket peatlands. *Soil Use Manage.* 27, 247–254.
- Wang, Y., Wang, S., Xue, B., Ji, L., Wu, J., Xia, W., Pan, H., Zhang, P., 1995. Sedimentological evidence of the piracy of the fossil Zoige lake by the Yellow River. *Chin. Sci. Bull.* 40, 1539–1544.
- Whittington, P.N., Price, J.S., 2006. The effects of water table draw-down (as a surrogate for climate change) on the hydrology of a fen peatland, Canada. *Hydrol. Process.* 20, 3589–3600.
- Wilson, L., Wilson, J., Holden, J., Johnstone, I., Armstrong, A., Morris, M., 2010. Recovery of water tables in Welsh blanket bog after drain blocking: discharge rates, time scales and the influence of local conditions. *J. Hydrol.* 391, 377–386.
- Xu, J.R., Morris, P.J., Liu, J.G., Holden, J., 2018. PEATMAP: refining estimates of global peatland distribution based on a meta-analysis. *Catena* 160, 134–140.
- Yang, G., Peng, C., Chen, H., Dong, F., Ning, W., Yang, Y., Zhang, Y., Zhu, D., He, Y., Shi, S., Zeng, X., Xi, T., Meng, Q., Zhu, Q., 2017. Qinghai-Tibetan Plateau peatland sustainable utilization under anthropogenic disturbances and climate change. *Ecosyst. Health Sustain.* 3, e01263. doi:10.1002/ehs01263.01263.
- Yu, K.F., Lehmkühn, F., Falk, D., 2017. Quantifying land degradation in the Zoige Basin, NE Tibetan Plateau using satellite remote sensing data. *J. Mountain Sci.* 14, 77–93.
- Zeng, M., Zhu, C., Song, Y., Ma, C., Yang, Z., 2017. Paleoenvironment change and its impact on carbon and nitrogen accumulation in the Zoige wetland, northeastern Qinghai-Tibetan Plateau over the past 14,000 years. *Geochem. Geophys. Geosyst.* 18, 1775–1792. <https://doi.org/10.1002/2016GC006718>.